Revista de Metalurgia
January-March 2023, 59 (1), e238
ISSN-L: 0034-8570
https://doi.org/10.3989/revmetalm.238

The influence of the ageing temperature on different properties of the EN AW-7075 aluminium alloy

Uroš Stamenković*, Svetlana Ivanov, Ivana Marković, Milan Gorgievski, Kristina Božinović, Avram Kovačević

University of Belgrade, Technical Faculty in Bor, Vojske Jugoslavije 12, Bor, Serbia
(*Corresponding author: ustamenkovic@tfbor.bg.ac.rs)

Submitted: 2 April 2022; Accepted: 18 March 2023; Available On-line: 27 April 2023

ABSTRACT: The influence of the ageing temperature on the hardness, electrical conductivity, thermal diffusivity and thermal conductivity of the EN AW-7075 aluminium alloy was studied in this paper. After solution treating the alloy at 480 °C for 1 h and quenching it in ice water, the investigated alloy was characterized using Differential Thermal Analysis (DTA) in order to determine the optimal temperatures for the isochronal ageing treatments. Afterwards, isochronal ageing was conducted at the temperature range of 110 °C-250 °C for 30 min The hardness, electrical conductivity, thermal diffusivity, thermal conductivity and microstructural features were investigated during the ageing treatments. Hardness had a peak value after ageing at 150 °C, while other properties gradually increased with the ageing temperature. Microstructural investigation of the aged alloy by SEM-EDS revealed the existence of precipitated phases that appear homogenously distributed in the microstructure.

KEYWORDS: Ageing; Electrical conductivity; EN AW-7075; Hardness; Thermal properties

Citation/Citar como: Stamenković, U.; Ivanov, S.; Marković, I.; Gorgievski, M.; Božinović, K.; Kovačević, A. (2023). "The influence of the ageing temperature on different properties of the EN AW-7075 aluminium alloy". *Rev. Metal.* 59(1): e238. https://doi.org/10.3989/revmetalm.238

RESUMEN: *Influencia de la temperatura de envejecimiento en diferentes propiedades de la aleación de aluminio EN AW-7075.* En este trabajo se estudió la influencia de la temperatura de envejecimiento sobre la dureza, la conductividad eléctrica, la difusividad térmica y la conductividad térmica de la aleación de aluminio EN AW-7075. Tras realizar un tratamiento de solubilización a 480 °C durante 1 h y templar la aleación en agua helada, se caracterizó mediante Análisis Térmico Diferencial (ATD) con el fin de determinar las temperaturas óptimas para los tratamientos de envejecimiento isócronos. A continuación, se llevó a cabo el envejecimiento isócrono a temperaturas comprendidas entre los 110 °C y los 250 °C durante 30 min Después de realizar estos tratamientos térmicos de envejecimiento, se determinó la dureza, y se caracterizó su conductividad eléctrica, la difusividad térmica, la conductividad térmica y las fases presentes en la microestructura. La dureza alcanzó un valor máximo tras el envejecimiento a 150 °C, mientras que las demás propiedades aumentaron gradualmente con la temperatura de envejecimiento. La caracterización microestructural mediante SEM-EDS de la aleación envejecida

reveló la existencia de fases precipitadas que aparecen homogéneamente distribuidas en la microestructura.

PALABRAS CLAVE: Envejecimiento; Conductividad eléctrica; EN AW-7075; Dureza; Propiedades térmicas

ORCID ID: Uroš Stamenković (https://orcid.org/0000-0002-7579-2159); Svetlana Ivanov (https://orcid.org/0000-0002-5326-0602); Ivana Marković (https://orcid.org/0000-0003-4431-9921); Milan Gorgievski (https://orcid.org/0000-0002-9899-719X); Kristina Božinović (https://orcid.org/0000-0002-9834-448X); Avram Kovačević (https://orcid.org/0000-0003-4009-4876)

1. INTRODUCTION

The EN AW-7075 aluminium alloy is one of the most used alloys in the automobile and aerospace industries as well as other various industries due to its very high strength, fatigue resistance, corrosion resistance, relatively high values of electrical and thermal conductivity. These good properties are mainly due to precipitation nanoscale phases during the ageing treatments (Fallahi *et al.*, 2013; Kacar and Guleryuz, 2015; Ozer and Karaaslan, 2017; Ku *et al.*, 2018; Pankade *et al.*, 2018; Padap *et al.*, 2020; Cai *et al.*, 2020; Sambathkumara *et al.*, 2021). The EN AW-7075 aluminium alloy is very susceptible to natural and artificial ageing treatments so properties of this alloy can be enhanced by precipitation hardening. The largely accepted precipitation sequence for this alloy can be presented as: $\alpha_{ssss} \rightarrow$ GP zones $\rightarrow$ metastable η' phase $\rightarrow$ stable η phase (Panigrahi and Jayaganthan, 2011; Kacar and Guleryuz, 2015; Choi *et al.*, 2015; Ozer and Karaaslan, 2017; Kilic *et al.*, 2019; Cai *et al.*, 2020). During the research of different mechanical properties, the authors focus on achieving the precipitation of a metastable η' phase. This phase is considered the most important in the precipitation sequence because it is responsible for hardening in this alloy. It is widely accepted in the literature that this phase has a hexagonal crystal structure, it is semi-coherent with the matrix and it usually precipitates on {111} planes (Ku *et al.*, 2018; Cai *et al.*, 2020). Nicolas (2002) stated in his dissertation that this phase can be presented as $MgZn_2$, but there is a strong possibility for copper to be present in this so-called η' phase. Many authors have focused their research on the mechanical properties of the EN AW-7075 aluminium alloy during different heat treatments (Panigrahi and Jayaganthan, 2011; Fallahi *et al.*, 2013; Kacar and Guleryuz, 2015; Chen *et al.*, 2015; Ozer and Karaaslan, 2017; Ku *et al.*, 2018; Kilic *et al.*, 2019; Cai *et al.*, 2020). Kacar and Guleryuz (2015) showed that the quench rate, pre-straining as well as the ageing temperature and time, play an important role in the precipitation hardening. Cai *et al.* (2020) applied the two-stage ageing process on the EN AW-7075 aluminium alloy. They achieved better strengthening through a two-stage ageing in comparison with the conventional ageing treatment. Ozer and Karaaslan (2017) showed a positive effect of the retrogression process on the tested samples. Ku *et al.* (2018) investigated the ductility after high temperature artificial ageing and reported higher values of ductility after this treatment in comparison with the samples' ductility after full annealing. Fallahi *et al.* (2013) tested the samples of the EN AW-7075 alloy before and after obtaining the ultra-fine grain structure by equal-channel angular pressing. They showed an increase in hardness values after achieving the ultra-fine grain structure. The change in the electrical conductivity during different heat treatments was investigated by Simsek *et al.* (2019). They reported a decrease in the electrical conductivity with an increase in ageing time (Simsek, 2019). Pankade *et al.* (2018) showed that both retrogression and re-ageing as well as duplex ageing provide higher values of electrical conductivity in comparison with the classical T6 ageing treatment. Some authors investigated the thermal properties of the EN AW-7075 aluminium alloy (Greb *et al.*, 2019; Padap *et al.*, 2020). Greb *et al.* (2019) reported an increase in the thermal diffusivity and thermal conductivity values with the increase in the temperature up to 600 °C for both the EN AW-7075 and the EN AW-6060 aluminium alloys, after applying continuous heating treatments to the investigated alloys. Padap *et al.* (2020) studied the effect of the ageing treatment and uniaxial compression on the thermal properties of the EN AW-7075 aluminium alloy. They reported an increase in the thermal conductivity values after ageing when compared with the solution heat treated samples, confirming the effect of ageing on the thermal properties. They also reported that the thermal conductivity was improved by 2.38% after compression and ageing when compared to the received sample (Padap *et al.*, 2020). After reviewing the current literature, it can be concluded that the ageing process can increase the hardness, the tensile strength, the toughness, even the ductility. Thermophysical properties, like the electrical conductivity, the thermal diffusivity and the thermal conductivity can be improved by using various ageing methods, including conventional and new ones. The investigations of the EN AW-7075 aluminium alloy are mostly based on the study of the influence of the isothermal ageing process (ageing time is changing at a constant temperature) on different properties, mainly mechanical properties. The focus of the isothermal ageing is to determine how long it would be necessary to age an alloy at certain temperatures in order to improve the investigated properties. Fan *et al.* (2021) showed that with an increase in the ageing temperature there is a possibility to achieve relatively high values of hardness but for shorter times. Therefore, our goal was to investigate the influence of temperature during ageing at a constant time (30 min) on the hardness, electrical conductivity, thermal diffusivity and thermal conductivity of the EN AW-7075 aluminium alloy. The aim of this investigation has been to produce satisfactory values of hardness by using the isochronal ageing regime that would include

the use of short ageing times in combination with higher ageing temperatures. Besides, the secondary goal was to achieve as high values of thermal properties as possible with the same ageing regime, because those properties are also important for higher temperature industry applications. Also, by using shorter ageing times at higher temperatures there is an important economic and ecological factor. Practical significance lies in the fact that the whole heat treatment process takes a shorter amount of time and requires less energy; therefore, it is more economically sustainable.

2. MATERIALS AND METHODS

The EN AW-7075 aluminium alloy was chosen for this experimental investigation. Extruded rounded bars from "AlCu metali d.o.o." company were delivered in peak aged condition. The chemical composition of the investigated alloy was determined by XRF analysis using a Bruker S1 Titan Handheld XRF Mod-800 analyser, and the obtained results are given in Table 1. The annealed condition was used as the first reference condition. This condition is referred to in the literature as temper *T-O* (the softest temper of wrought products). In order to achieve this condition, all samples were annealed at 480 °C for 3 h (denoted as T-O sample) in the electric resistance furnace Vims elektrik LPŽ-7,5 S and subsequently cooled in still air. After this treatment, all investigated properties are measured and referenced in graphs. Samples in T-O condition were again heated with a rate of 8 °C·min^{-1} to a temperature of 480 °C and held at that temperature for 1 h. In order to achieve the super saturated solid solution state (α_{ssss}), quenching in ice water was performed after these heat treatments (denoted as T-W sample). Due to the quench rate sensitivity of this alloy, the ice bath was moved as close as possible to the furnace to minimize the transfer time (avoid temperature loss) and prevent precipitation during cooling. The quenched samples were then subjected to isochronal ageing at the temperature range of 110 °C-250 °C for 30 min each. All quenched samples were held in an ice bath to temperatures below 0 °C in order to avoid the influence of natural ageing.

Table 1. XRF analysis of the EN AW-7075 alloy (mass.%)

Zn	Mg	Cu	Si	Fe
5.61	2.77	1.55	0.17	0.31
Cr	**Ti**	**Mn**	**Other**	**Al**
0.21	0.02	0.18	0.07	89.11

The quenched sample was characterized using differential thermal analysis (DTA) using the SDT Q600 (TA Instruments) analyser with heating rate of 10 °C·min^{-1} up to 450 °C. Xenon flash method was applied to determine the thermal diffusivity of the investigated alloy after ageing by irradiating the disc shaped specimens (with a diameter of 12.7 mm) with the xenon lamp in a nitrogen atmosphere. The thermal conductivity was calculated according to the equation:

$$\lambda(T) = \rho(T) \times c_p(T) \times \alpha(T) \quad (1)$$

where, λ - thermal conductivity (W/m·K), ρ – density (kg×m^{-3}), c_p – specific heat capacity (J/kg·K), α - thermal diffusivity (m^2×s^{-1}), T – temperature (K). Electrical conductivity was measured using the electrical conductivity tester Sigmatest 2.063. Vickers hardness was measured using a VEB Leipzig hardness tester with a 15 kg load and a 15 s dwelling time and following the ASTM E384-22 (2022). For the investigation of phases present in the microstructure and their distribution, the TESCAN Vega 3 LMU scanning electron microscope equipped with the X - ray EDS detector by Oxford Instruments was used. The preparation of the samples included wet grinding on a series of SiC papers and polishing with alumina slurry with two different Al_2O_3 particle sizes (0.3 μm and 0.05 μm). Dix-Keller reagent was used to etch the samples by immersing them for around 2 min to reveal fine dispersed particles.

3. RESULTS AND DISCUSSION

a. The differential thermal analysis (DTA)

From the Fig. 1, it can be seen that one wide peak appears at around 200 °C. Based on the literary data (Panigrahi and Jayaganthan, 2011; Ku *et al.*, 2018; Hebbar *et al.*, 2020) and the appearance of one wide DTA peak at around 200 °C, it can be concluded that this peak represents the precipitation range of the metastable η' phase. Due to the wideness of the peak, it can be assumed that some other phases will precipitate in that temperature range, i.e., GP zones (a tempera-

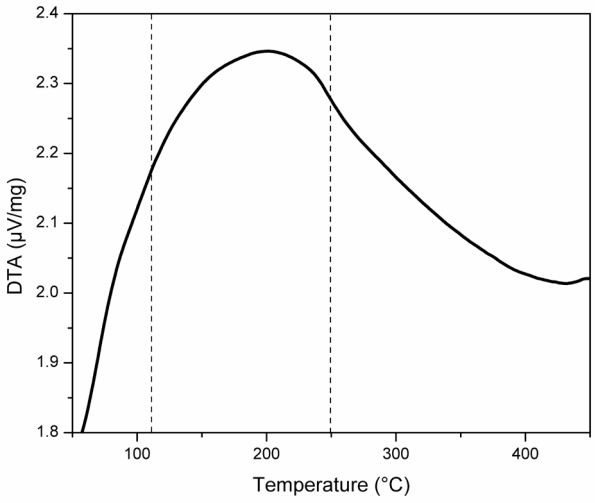

Figure 1. Differential thermal analysis (DTA) curve of the EN AW-7075 aluminium alloy.

tures lower than 200 °C). Based on the DTA curve, the temperature range of the ageing regime was defined (110 °C – 250 °C).

b. Investigation of the hardness

Figure 2 shows the change in hardness values as a function of the ageing temperature during the isochronal ageing for 30 min The hardness gradually increases with the ageing temperature, reaching the maximum value of 158 ± 5 HV_{15} after ageing for 30 min at 150 °C. The hardness values obtained for all aged samples are higher in comparison with the quenched sample (98 ± 3 HV_{15}). Similar results were reported by other authors (Fan *et al.*, 2021). These results confirm that the EN AW-7075 aluminium alloy has a very good response to this type of ageing treatment. The hardness peak obtained appears in the temperature range where the DTA peak appeared (Fig. 1). However, the tip of the DTA peak is shifted to a higher temperature compared to the hardness peak due to the factors such as: low calorimetric effect, sample size, heating rate and factors concerning measuring equipment (furnace atmosphere, type of sample holders, sensitivity of the recording system etc.). It should be borne in mind that diffusionally activated phase transformations, like the precipitation reactions, significantly affect the heating rate. Somewhat similar results were obtained by other authors (Panigrahi and Jayaganthan, 2011; Ku *et al.*, 2018; Hebbar *et al.*, 2020; Liu *et al.*, 2020).

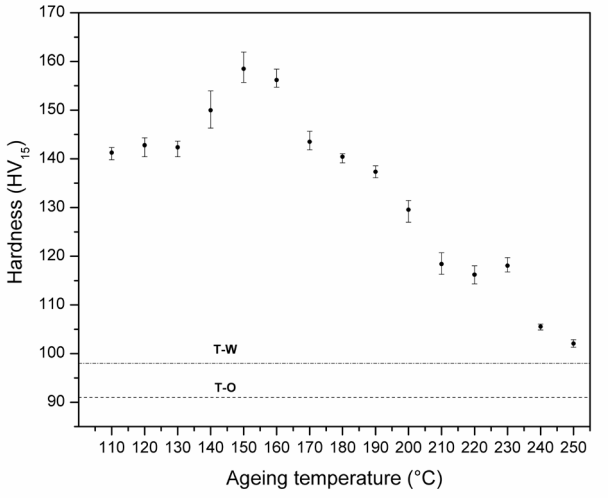

Figure 2. Hardness values of the EN AW-7075 alloy after the isochronal ageing treatment for 30 min

Up to the temperature of 130 °C, the increase in hardness values is significant in comparison with the quenched sample. At these ageing temperatures, the formation of the GP zones occurs and the interaction with the moving dislocations starts. GP zones are coherent with the aluminium matrix; therefore, dislocations either cut them or lock onto them. During this process the surface energy increases and the kinetic energy of the dislocations is spent, causing the hardness of the investigated alloy to increase as it is seen in Fig. 2. Siddiqui *et al.* (2000) confirmed that the higher the ageing temperature and time, the faster the formation kinetics of the GP zones and the larger their density were. As the ageing temperature increases, the GP zones start to transform into the metastable η' phase. It can be assumed that there is a temperature range where GP zones and metastable η' phase coexist. The dissolution of GP zones and nucleation of the metastable η' phase is a diffusion driven process that needs higher temperatures and longer times to complete. Therefore, the increase in the hardness values and the achievement of the peak hardness after ageing at 150 °C for 30 min is due to the existence of these hardening phases, i.e., GP zones and the metastable η' phase. The metastable η' phase is semi-coherent with the aluminium matrix and, therefore, a small lattice distortion is expected. With this distortion, several slip systems begin to appear that cause the accumulation of a larger number of dislocations. Dislocations are inhibited by the newly formed η' precipitates and they accumulate at grain boundaries, leading to the highest hardness values (Sha and Cerezo, 2004; Yang *et al.*, 2014; Kacar and Guleryuz, 2015; Ozer and Karaaslan, 2017; Cai *et al.*, 2020). Dislocation accumulation and inhibition at grain boundaries can be viewed in two ways: 1) grain boundaries are obstacles to dislocation movement; if the dislocation does not surpass the grain boundaries, it will accumulate at them (Pan *et al.*, 2021); 2) grain boundaries are an excellent heterogenous site for the nucleation of phases, so it can be assumed that the η' and other precipitates nucleate at the grain boundaries, also causing the hindering of dislocation movement (Goswami *et al.*, 2013). With the increase of the ageing temperature above 160 °C, the hardness decreases due to the gradual disappearance of GP zones and the coarsening of the η' precipitates. In addition, upon reaching the ageing temperature of 230 °C, it can be assumed that the formation of the stable η phase ($MgZn_2$) starts. This stable phase is incoherent with the Al matrix, but in the early stages of formation, it can be assumed that the precipitates are fine and evenly dispersed so the increase in hardness values up to 230 °C can be explained in this way. Afterwards, the hardness values decrease, reaching the values obtained for the quenched samples due to over-ageing and the coarsening of the stable η precipitates (Mukhopadhyay *et al.*, 1994; Kacar and Guleryuz, 2015; Kilic *et al.*, 2019). These processes cause the relaxation of the Al matrix, the easier movement of dislocations and, thus, lower values of hardness.

c. Investigation of the electrical conductivity

Essentially, there are two processes caused by precipitation: 1) the depletion of the matrix which causes relaxation and easier movement of electrons, thus

increasing the electrical conductivity; 2) the appearance of metastable precipitates (GP zones, η' precipitates) that distort the matrix causing the scattering of electrons, thus decreasing the electrical conductivity. Which of these two processes is more active, directly determines the behaviour of electrical conductivity at a given heat treatment conditions.

In the temperature range of 110 °C - 170 °C aged samples have a lower electrical conductivity values in comparison with the quenched sample. The minimum electrical conductivity value was detected after ageing at 140 °C. Lower values of the electrical conductivity in this temperature range are due to the formation of the GP zones and early stage η' precipitates formation. The existence of these precipitates causes the scattering of electrons (process number 2 dominates). Scattering then causes the rise of the electrical resistance and therefore, a decrease in electrical conductivity. Coherency and semi-coherency of GP zones and early stage η' precipitates formation, respectively, are causing the appearance of stress fields in the crystal lattice, which leads to an increase in the electrical resistance (Ozer and Karaaslan, 2017). After the initial decrease, the electrical conductivity gradually increases as the ageing continues, and the matrix gets less saturated (loses the quenched-in elements). Salazar-Guapuriche *et al.* (2006) suggested that almost all alloying elements increase the electrical resistance when they are in solid solution (as-quenched condition after the solution treatment). A lower saturation of the matrix in alloying elements gives higher values of the electrical conductivity, as it is seen in Fig. 3, after ageing above 170 °C. After ageing at the temperatures above 170 °C it can be concluded that there is a gradual disappearance of GP zones and the coarsening of the η' precipitates, causing the process number 1 to dominate. In addition, the highest values of the electrical conductivity are obtained due to over-ageing of the investigated alloy similar to the works of Pankade *et al.* (2018) and Simsek (2019). As the over ageing leads to the decrease in the hardness values, in this case it leads to an increase in the electrical conductivity, as concluded by Ozer and Karaaslan, (2017). Khangholi *et al.* (2021) explained in his paper that the electrical conductivity decreases due to the sum of different contributions of various microstructural defects that cause electron scattering. It can be assumed that, due to over-ageing, a stable η phase is present in the microstructure. This phase is incoherent with the matrix so the electron scattering effect is low and is dominated by process number 1 (strong precipitation from the matrix). This can be seen on Fig. 2 and Fig. 3 after ageing at 230 °C for 30 min At that temperature, even though the η phase is coherent with the matrix, some distortion is surely present in the matrix, causing hardness values to increase and electrical conductivity to decrease.

d. Investigation of the thermal properties

Figures 4 and 5 show the influence of ageing temperature on the thermal diffusivity and thermal conductivity values of the investigated alloy, respectively, during the isochronal ageing for 30 min

Since the thermal properties, as well as the electrical ones, depend on the electron flow, the presented diagrams in Figs. 4 and 5 are somewhat similar to the one given for the electrical conductivity (Fig. 3). Observing the presented diagrams, it can be concluded that by ageing the alloy in the temperature range from 110 °C to 180 °C, the values of thermal diffusivity and thermal conductivity are below the value of the quenched sample. In this temperature range, GP zones and other type of precipitates are active and are responsible for the scattering of electrons, but also serve as obstacles to the movement of heat (Edwards *et al.*, 1998; Lumley *et al.*, 2013; Cui *et al.*, 2014).

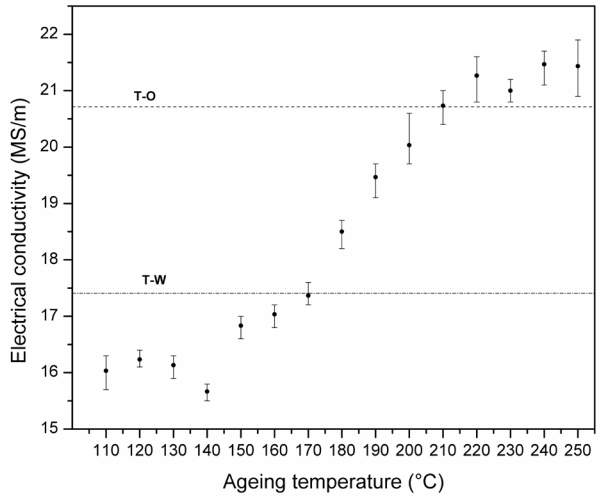

Figure 3. Electrical conductivity values of the EN AW-7075 alloy after the isochronal ageing treatment for 30 min

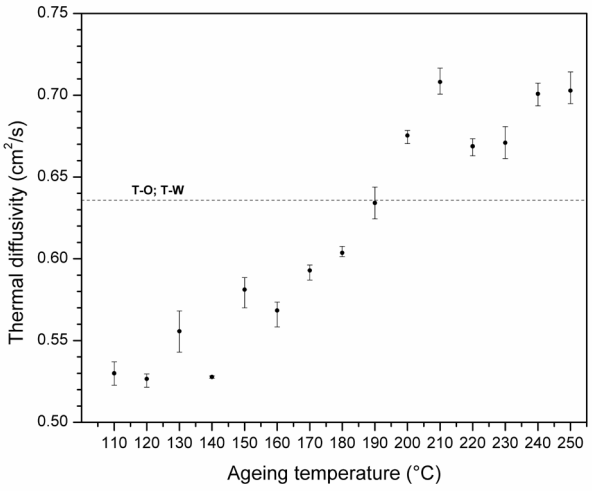

Figure 4. Thermal diffusivity values of the EN AW-7075 alloy after the isochronal ageing treatment for 30 min

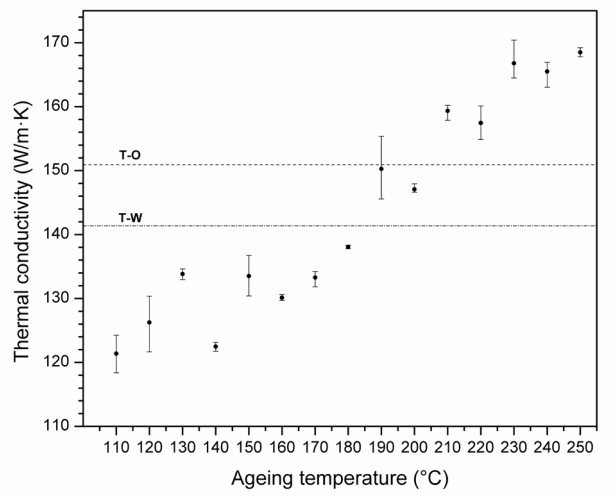

Figure 5. Thermal conductivity values of the EN AW-7075 alloy after the isochronal ageing treatment for 30 min

With an increase in ageing temperature (190 °C-250 °C), the values of thermal diffusivity and thermal conductivity of the aged samples are higher compared to the quenched sample. The reason for this can be found in the activation and easier movement of electrons. The increase in the ageing temperature leads to more intensive precipitation, transformation and decomposition of GP zones, and thus the formation of a metastable semi-coherent η' phase. All this, together with the constant impoverishment of the solid solution, clears the way for the movement of electrons, increasing the values of thermal properties. Padap *et al.* (2020) also obtained higher values of thermal conductivity after ageing in comparison with the quenched state. Greb *et al.* (2019) had an increase in thermal conductivity and diffusivity values around 200 °C after continuous heating the EN AW-7075 alloy.

e. Microstructural investigation

A more detailed study of the microstructural changes during the isochronal ageing was performed using SEM-EDS analyses. The peak aged sample with the highest hardness value (aged at 150 °C for 30 min) was selected for this analysis. Figure 6 shows different sites of interests in the peak aged sample, at different magnifications. Precipitated particles and their chemical compositions were investigated and the results of the investigation are given in Fig. 6 and Tables 2-4.

Spectrum S1 in Fig. 6a (Table 2) and spectrum S3 in Fig. 6b (Table 3) indicate the presence of Al_2Cu phase in the aged samples. Dos Santos *et al.* (2021) stated that this phase appears in a white colour after etching the sample with Dix-Keller solution as in this investigation. Similar results were obtained by Chen *et al.* (2015) and Ku *et al.* (2018). The S2 spectrum in Fig. 6a (Table 2) may indicate the presence of the Al_7Cu_2Fe phase, which remained undissolved in the solid solu-

Table 2. Chemical composition of the analysed spectrums (at.%) shown in Fig. 6a

Spectrum	Mg	Al	Fe	Cu	Zn
S1	0	63.73	3.57	32.7	0
S2	0	80.72	9.48	9.8	0
S3	4.37	91.26	2.43	1.93	0
S4	3.63	94.59	0	0	1.79

Table 3. Chemical composition of the analysed spectrums (at. %) shown in Fig. 6b

Spectrum	Mg	Al	Fe	Cu	Zn
S1	3.38	92.63	0	0	3.98
S2	2.92	89.88	0	7.2	0
S3	3.41	69.73	0	26.86	0

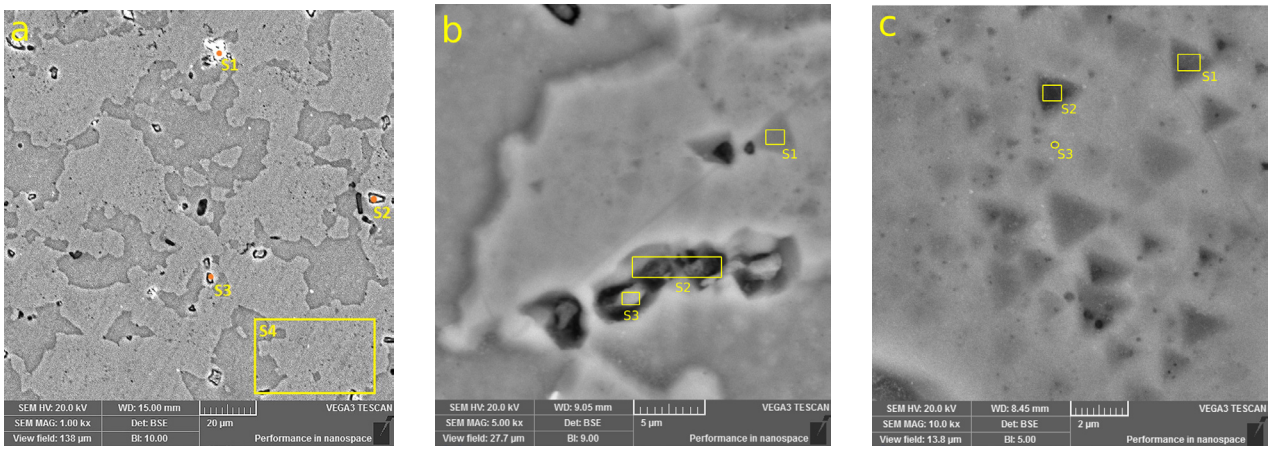

Figure 6. SEM and EDS analyses of the EN AW-7075 alloy after ageing at 150 °C for 30 minutes: a) site of interest 1, x1000; b) site of interest 2, x5000; c) site of interest 3, x10000.

tion by previous annealing. The spectrum S3 in Fig. 6a (Table 2) and spectrum S2 in Fig. 6b (Table 3) probably indicates the existence of the Al_2CuMg phase (sometimes denoted in literature as S-phase). The presence of this phase is also mentioned by other authors. Woznicki *et al.* (2021) mentioned the existence of this phase after the homogenization of the cast EN AW-7075 aluminium alloy, while MacKenzie (2000) obtained this phase after quenching and obtaining the super saturated solid solution. From Fig. 6a-b and Table 2-3, it can be seen that particles containing Cu sometimes precipitate on grain boundaries. An analysis of the large scanning area given by the spectrum S4 in Fig. 6a (Table 2) shows the presence of Al, Mg and Zn, which can indicate that the whole scanning area is covered with finely distributed metastable η' phase ($MgZn_2$). The scanning area, like the one represented with spectrum S4 in Fig. 6a, was magnified to the magnification of x10000 and analysed (Fig. 6c, Table 4). From the presented Fig. 6c it can be seen that the whole area is covered by small precipitates. Some precipitates have triangular and some plate-like shapes. EDS analysis was performed on both types of precipitates (spectrums S1-S3, Fig. 6c). The obtained results cannot confirm the exact proportion of the magnesium and zinc in this phase, but from the analysis of the obtained spectrums and Table 4, it can be assumed that those particles represent the η' phase ($MgZn_2$). Ultra-fine particles of this phase are very difficult to detect at these magnifications; however, hardness results obtained for the sample aged at 150 °C for 30 min indirectly anticipate their presence.

Table 4. Chemical composition of the analysed spectrums (at. %) shown in Fig. 6c

Spectrum	Mg	Al	Cu	Zn
S1	3.33	91.07	1.91	3.69
S2	3.35	90.86	1.85	3.94
S3	3.04	93.56	0	3.4

4. CONCLUSIONS

Conclusions in this paper can be summarized as:

- The DTA analysis revealed one wide peak at around 200 °C. This peak can be ascribed to the precipitation of the metastable/stable phases.
- Hardness values significantly increased during isochronal ageing. Peak aged sample reached the hardness value of 158 ± 5 HV_{15} after ageing at 150 °C for 30 min After peak ageing, hardness increased 61.2% in comparison to the quenched sample.
- Until the temperature reaches 170 °C, electrical conductivity values are lower than those obtained after quenching. After that, electrical conductivity gradually increases until it reaches its maximum after ageing at 240 °C for 30 min The maximal obtained value is 23.6% higher in comparison to the value obtained for the quenched sample.
- Thermal diffusivity and conductivity are influenced by the precipitation during the isochronal ageing. Up to about 190 °C, values of thermal diffusivity and conductivity are lower than those obtained for the quenched sample, and after that they gradually increase until they reach maximum values. At maximum value, thermal diffusivity was increased by 11.6% and thermal conductivity by 16.9% compared to the quenched sample.

The highest hardness values observed in the literature by conventional isothermal ageing (for low ageing temperature at long ageing time) cannot be obtained using high temperature ageing with shorter ageing time. However, in electrical and machining industry applications it is not necessary to have the highest possible hardness, but to have optimal values of different mechanical and thermophysical properties. At the peak hardness condition, the highest values of electrical conductivity, thermal diffusivity and thermal conductivity were not achieved. Although, after ageing at 190 °C – 200 °C for 30 min, the hardness values were around 135 ± 3 HV_{15} and values of the electrical conductivity, the thermal diffusivity and the thermal conductivity were almost as high as those for the T-O condition. The obtained results indicate that there may be a use for such ageing treatment in electrical industry. An additional example would be the use of the EN AW-7075 alloy in making anodes for air batteries. In this application, the movement of electrons can be of importance, so high electrical and thermal conductivity are strongly beneficial to this type of industrial application. Also, machining the parts made of aluminium alloys is especially difficult due to the local melting caused by tool friction. In this application, thermal conductivity in combination with relatively high values of hardness facilitates machining. Given that, this ageing regime produces satisfactory optimal values of hardness, electrical conductivity, thermal diffusivity and thermal conductivity, and it can be used in industrial settings where economic and ecological factors are of utmost importance. This is due to the fact that with this ageing treatment, optimal values of the investigated properties are achieved after only 30 min, which saves time and energy.

ACKNOWLEDGMENTS

The research presented in this paper was done with the financial support of the Ministry of Science, Technological Development and Innovation of the Republic of Serbia, within the funding of the scientific research work at the University of Belgrade, Technical Faculty in Bor, according to the contract with registration number 451-03-47/2023-01/200131.

REFERENCES

ASTM E384-22 (2022). Standard Test Method for Microindentation Hardness of Materials. ASTM International, West Conshohocken, PA, USA.

Cai, S.W., He, Y., Song, R.G. (2020). Study on the Strengthening Mechanism of Two-Stage Double-Peaks Aging in 7075 Aluminum Alloy. *Trans. Indian Iinst. Met.* 73 (1), 109-117. https://doi.org/10.1007/s12666-019-01809-7.

Chen, G., Chen, Q., Wang, B., Du, Z.-M. (2015). Microstructure evolution and tensile mechanical properties of thixoformed high performance Al-Zn-Mg-Cu alloy. *Met. Mater. Int.* 21 (5), 897-906. https://doi.org/10.1007/s12540-015-5139-6.

Choi, S.W. Cho, H.S., Kang, C.S., Kumai,S. (2015). Precipitation dependence of thermal properties for Al–Si–Mg–Cu–(Ti) alloy with various heat treatment. *J. Alloys Compd.* 647, 1091-1097. https://doi.org/10.1016/j.jallcom.2015.05.201.

Cui, L., Liu, Z., Zhao, Xi., Tang, J., Liu, K., Liu, X., Qian, C. (2014). Precipitation of metastable phases and its effect on electrical resistivity of Al-0.96Mg_2Si alloy during aging. *Trans. Nonferrous. Met. Soc. China* 24 (7), 2266-2274. https://doi.org/10.1016/S1003-6326(14)63343-4.

Dos Santos, S.L., Toloczko, F.R., Merij, A.C., Saito, N.H., Da Silva, D.M. (2021). Investigation and Nanomechanical Behavior of the Microconstituents of Al-Si-Cu alloy After Solution and Ageing Heat Treatments. *Mater. Res.* 24 (2), e20200329. https://doi.org/10.1590/1980-5373-MR-2020-0329.

Edwards, G.A., Stiller, K., Dunlop, G.L., Couper, M.J. (1998). The precipitation sequence in Al–Mg–Si alloys. *Acta Mater.* 46 (11), 3893-3904. https://doi.org/10.1016/S1359-6454(98)00059-7.

Fallahi, A., Hosseini-Tudeshky, H., Ghalehbandi, S.M. (2013). Effect of heat treatment on mechanical properties of ECAPed 7075 aluminum alloy. *Adv. Mat. Res.* 829, 62-66. https://doi.org/10.4028/www.scientific.net/AMR.829.62.

Fan, Y., Tang, X., Wang, S., Chen, B. (2021). Comparisons of Age Hardening and Precipitation Behavior in 7075 Alloy Under Single and Double-Stage Aging Treatments. *Met. Mater. Int.* 27, 4204-4215. https://doi.org/10.1007/s12540-020-00875-7.

Goswami, R., Lynch, S., Holroyd N.J.H., Knight, S.P., Holtz R.L. (2013). Evolution of Grain Boundary Precipitates in Al 7075 Upon Aging and Correlation with Stress Corrosion Cracking Behavior. *Metall. Mater. Trans. A.* 44, 1268-1278. https://doi.org/10.1007/s11661-012-1413-0.

Greb, T., Mittler, T., Schmid, S., Volk, W., Chen, H., Khalifa, N.B. (2019). Thermal analysis and production of As-Cast Al 7075/6060 Bilayer billets. *Int. J. Metalcast.* 13 (4), 817-829. https://doi.org/10.1007/s40962-018-0282-8.

Hebbar, S., Kertsch, L., Butz, A. (2020). Optimizing Heat Treatment Parameters for the W-Temper Forming of 7xxx Series Aluminum Alloys. *Metals* 10 (10), 1361. https://doi.org/10.3390/met10101361.

Kacar, R., Guleryuz, K. (2015). Effect of Quenching Rate and Pre-strain on the Strain Ageing Behaviors of 7075 Aluminum Alloys. *Mater. Res.* 18 (2), 328-333. https://doi.org/10.1590/1516-1439.307414.

Khangholi, S.N., Javidani, M., Maltais, A., Chen, X. (2021). Effects of natural aging and pre-aging on the strength and electrical conductivity in Al-Mg-Si AA6201 conductor alloys. *Mater. Sci. Eng. A.* 820, 141538. https://doi.org/10.1016/j.msea.2021.141538.

Kilic, S., Kacar, I., Sahin, M., Ozturk, F., Erdem, O. (2019). Effects of Aging Temperature, Time, and Pre-Strain on Mechanical Properties of AA7075. *Mater. Res.* 22 (5), e20190006. http://doi.org/10.1590/1980-5373-mr-2019-0006.

Ku, M.H., Hung, F.Y., Lui, T.S., Lai, J.J. (2018). Enhanced Formability and Accelerated Precipitation Behavior of 7075 Al Alloy Extruded Rod by High Temperature Aging. *Metals.* 8 (8), 648. https://doi.org/10.3390/met8080648.

Liu, Y., Zhu, B., Wang, Y., Li, S., Zhang, Y. (2020). Fast solution heat treatment of high strength aluminum alloy sheets in radiant heating furnace during hot stamping. *Int. J. Lightweight Mater.* 3 (1), 20-25. https://doi.org/10.1016/j.ijlmm.2019.11.004.

Lumley, R.G., Deeva, N., Larsen, R., Gemberovic, J., Freeman J. (2013). The Role of Alloy Composition and T7 Heat Treatment in Enhancing Thermal Conductivity of Aluminum High Pressure Diecastings. *Metall. Mater. Trans. A.* 44 (2), 1074–1086. https://doi.org/10.1007/s11661-012-1443-7.

MacKenzie, D.S. (2000). *Quench rate and ageing effects in aluminum-zinc-magnesium-copper aluminum alloys.* PhD Thesis, Faculty of the Graduate School of the University of Missouri-Rolla, Missouri, USA. https://www.researchgate.net/publication/241318106.

Mukhopadhyay, A.K., Yang, Q.B., Singh, S.R. (1994). The influence of zirconium on the early stages of aging of a ternary Al-Zn-Mg alloy. *Acta Metall. Mater.* 42 (9), 3083-3091. https://doi.org/10.1016/0956-7151(94)90406-5.

Nicolas, M. (2002). *Precipitation evolution in an Al-Zn-Mg alloy during non-isothermal heat treatments and in the heat-affected zone of welded joints*. PhD Thesis, The Grenoble Institute of Technology, Grenoble, France. https://tel.archives-ouvertes.fr/tel-00370436.

Ozer, G., Karaaslan, A. (2017). Properties of AA7075 aluminum alloy in aging and retrogression and reaging process. *Trans. Nonferrous. Met. Soc. China* 27 (11), 2357-2362. https://doi.org/10.1016/S1003-6326(17)60261-9.

Padap, A.K., Yadav, A.P., Kumar, P., Kumar, N. (2020). Effect of aging heat treatment and uniaxial compression on thermal behavior of 7075 aluminum alloy. *Mater. Today: Proc.* 33 (8), 5442-5447. https://doi.org/10.1016/j.matpr.2020.03.196.

Pan, H., Yue, H., Zhang, X. (2021). Interactions between Dislocations and Boundaries during Deformation. *Materials* 14 (4), 1012. https://doi.org/10.3390/ma14041012.

Panigrahi, S.K., Jayaganthan, R. (2011). Effect of Annealing on Thermal Stability, Precipitate Evolution, and Mechanical Properties of Cryorolled Al 7075 Alloy. *Metall. Mater. Trans. A.* 42 (10), 3208-3217. https://doi.org/10.1007/s11661-011-0723-y.

Pankade, S.B., Khedekar, D.S., Gogte, C.L. (2018). The influence of heat treatments on electrical conductivity and corrosion performance of AA 7075-T6 aluminium alloy. *Procedia Manuf.* 20, 53-58. https://doi.org/10.1016/j.promfg.2018.02.007.

Sha, G., Cerezo, A. (2004). Early-stage precipitation in Al–Zn–Mg–Cu alloy (7050). *Acta Mater.* 52 (15), 4503-4516. https://doi.org/10.1016/j.actamat.2004.06.025.

Salazar-Guapuriche, M.A., Zhao, Y.Y., Pitman, A., Greene, A. (2006). Correlation of Strength with Hardness and Electrical Conductivity for Aluminium Alloy 7010. *Mater. Sci. Forum.* 519-521, 853-858. https://doi.org/10.4028/www.scientific.net/MSF.519-521.853.

Sambathkumara, M., Sasikumara K.S.K., Gukendrana R., Dineshkumara K., Ponappab K., Harichandran S. (2021). Investigation of mechanical and corrosion properties of Al 7075/Redmud metal matrix composite. *Rev. Metal.* 57 (1), e185. https://doi.org/10.3989/revmetalm.185.

Siddiqui, R.A., Abdullah, H.A., Al-Belushi, K.R. (2000). Influence of aging parameters on the mechanical properties of 6063 aluminium alloy. *J. Mater. Process. Technol.* 102 (1-3), 234-240. https://doi.org/10.1016/S0924-0136%2899%2900476-8.

Simsek, I. (2019). Investigation of the effect of second phase precipitates on the corrosion and electrical conductivity of 7075 aluminum alloys. *Anti-Corros. Method. M.* 66 (5), 683-688. https://doi.org/10.1108/ACMM-02-2019-2082.

Woznicki, A., Leszczynska-Madej, B., Wloch, G., Grzyb, J., Madura, J., Lesniak, D. (2021). Homogenization of 7075 and 7049 Aluminium Alloys Intended for Extrusion Welding. *Metals* 11 (2), 338. https://doi.org/10.3390/met11020338.

Yang, X., Liu, J., Chen, J., Wan, C., Feng, L., Liu, P., Wu, C. (2014). Relationship Between the Strengthening Effect and the Morphology of Precipitates in Al–7.4Zn–1.7Mg–2.0Cu Alloy. *Acta Metall. Sin.* 27, 1070–1077. http://doi.org/10.1007/s40195-014-0122-7.